
Measuring collective behaviour of multicellular ensembles: role of space–time scales

S RAJESH and SOMDATTA SINHA*

Centre for Cellular and Molecular Biology, Uppal Road, Hyderabad 500 007, India

*Corresponding author (Fax, +91-40-27160591; Email, sinha@ccmb.res.in)

Living systems are spectacular examples of spatiotemporally organized structures. During the development of complex organization there is dynamic equilibrium between the local and global processes acting at the intra- and intercellular levels in multiple space and time scales. Although in modelling studies such spatiotemporal systems can be described by different space–time scales and at many organizational levels, the experimental quantities measured and predictions useful for practical applications are at a macroscopic (coarser or averaged) level/scale; these are limited by the resolution of the measuring method and experimental protocol. In this work, we address whether the spatiotemporal collective dynamics exhibited by a multiscale system can discriminate between, or be borne out by, the coarse-grained and averaged measurements done at different spatial and temporal scales. Using a simple model of a ring of cells, we show that measurements of both spatial and spatiotemporal average behaviour in this multicellular ensemble can mask the variety of collective dynamics observed at other space–time scales, and exhibit completely different behaviours. Such outcomes of measurements can lead to incomplete and incorrect understanding of physiological functions and pathogenesis in multicell ensembles.

[Rajesh S and Sinha S 2008 Measuring collective behaviour of multicellular ensembles: role of space–time scales; *J. Biosci.* **33** 289–301]

1. Introduction

Multicellular ensembles constitute groups of many cells. In a population, the individual behaviour of the cells may be uncorrelated and the population behaviour is a simple sum of the individual behaviours. When cells in a population interact, the individual behaviour of the cells is regulated by the interaction, and the ensemble can show a unified collective behaviour, which is not just a “sum of the parts”. Interactions can occur through the response of the individual cells in a population to a concentration of external molecules in their environment. Examples are the Community effect, Quorum sensing and Biofilms, where a population of similar cells exhibits cell density-dependent induction of new gene expression in response to an external signal

factor (Fuqua *et al* 1996; Miller and Bassler 2001; Freeman and Gurdon 2002; Costerton 2004; Garcia-Ojalvo *et al* 2004). Cells in tissues and organs are examples of structured ensembles of cells, which interact directly through membrane-bound molecules, gap junctions, diffusion of secreted chemicals, etc. (Suguna and Sinha 2005). The cardiac and muscle tissues, islets of Langerhans in the pancreas, plant roots, etc. are a few examples of the varied types of structures that are formed in this type of multicellular ensemble (Murray 1989). Here, the arrangement of cells and the types of contacts complement their specific functions. The collective dynamics of structured multicellular ensembles may have both space and time components giving rise to spatiotemporal dynamics and patterns.

Keywords. Collective behaviour; multiscale modelling; spatiotemporal dynamics; synchronization

Abbreviations used: CS, Complete synchronization; IPS, intermittent phase synchronization; PS, phase synchronization; TW, travelling wave

Multicellular ensembles are “multiscale systems”, i.e. they contain components that span multiple length and time scales. At the individual cell level, a complex intracellular network of interacting biochemical pathways governs the functional behaviour of the cells. Intercellular communication is a necessary prerequisite for effective collective functioning in multicellular ensembles. Emergence of the observed macroscopic (collective) behaviour arises from the type and strength of the interactions among the constituent cells and their local cellular behaviour. Thus, the average behaviour of the cellular ensemble is a result of both intra- and intercellular processes that happen at different space and time scales (Alarcon *et al* 2005). Biological function can also be studied at multiple levels, i.e. at different levels of abstraction (molecular, genetic, cellular, organismal, social/ecological). For example, the collective behaviour of chemotaxis in bacterial populations provides an example of how cell-level decision-making (signal detection, transduction and swimming behaviour) translates into population-level behaviour spanning time scales from 10^{-2} s to days (Erban and Othmer 2005). The role of intrinsic and extrinsic stochasticity and interaction with the environment at different organizational levels also has significant effects on the functioning of these ensembles (Sinha 2005; Maithreye and Sinha 2007). Given the multiscale and multilevel nature of biological processes, when a study is focused on a specific level/scale based on the question to be addressed, an important question that arises is whether the net effect of the smaller–faster scales on the larger–slower scales can be measured when studied at the specific larger–slower scales. Or, in other words, *how much information can get truncated or*

unresolved at some scale resulting in the loss of predictability at other scales.

Important information can also be lost when, in a spatiotemporal process, measurements are made only in any one dimension – either spatial or temporal. An example (G Myers, personal communication; Peng *et al* 2007) is shown in figure 1, where the expression of two genes (gene 1 and gene 2) has been studied by measuring their mRNA abundance levels for 12 h in whole *Drosophila* embryos. The temporal expression profiles of gene 1 and gene 2 (line plots in figure 1) indicate that the average expression levels of the two genes in whole embryos during specific developmental phases are highly correlated (correlation coefficient is 0.98). The insets in both the plots show the spatial pattern of expression of the two genes in the embryos at three different times, and it is very clear that their spatial expression pattern over time is totally uncorrelated. This example shows how, during experimentation, absence/truncation (spatial averaging) of information at the spatial scale can lead to a loss of information at the temporal scale leading to incomplete or even incorrect inferences with regard to co-expressions of the two genes during development.

Modelling multilevel/multiscale processes poses difficult mathematical and computational problems, and is an active area of research. To incorporate individual-level behaviour into population-level models, through the combination of microscopic description with macroscopic changes on a coarse grid, involves the use of different types of mathematics for their descriptions: continuous time Markov processes, discrete mechanics, continuum mechanics, discrete time processes, etc. (Garcia *et al* 1999; Shenoy *et al* 1999; Kevrekidis *et al* 2003; Setayeshagar *et al* 2005). In modelling biological

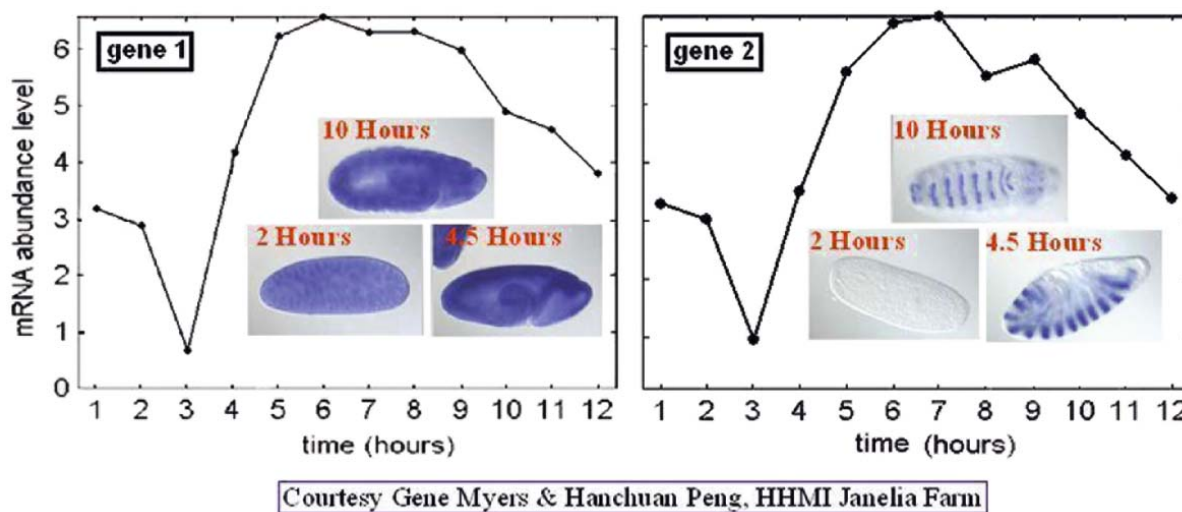


Figure 1. Measurement of the expression (mRNA abundance levels) of two genes showing their average temporal expression profile (line plot) and their spatiotemporal expression (inset).

processes, traditionally first the macroscopic evolution equations for each variable of importance is derived from the microscopic processes based on the existing experimental information. Different mathematical and computational tools are then used to derive the macroscopic descriptions. The implication is that the macroscopic rules, a description of the system at a coarse-grained, higher level of organization, can be deduced from the microscopic rules (Kevrekidis *et al* 2005). But, in general, the questions of interest that require practical answers are asked at the macroscopic (“system”) scale, whereas the multicomponent model description is at a much finer scale, which can be explicitly tracked in a simulation. Sometimes the level of observation at which one can be practically predictive is also unclear. Thus, while extending the modelling and simulation results to experimental observations, it is necessary to be aware of this gap between the two. The inferences drawn would be only as good as the data on which they are based which, in turn, depend on the important problem of “resolution” and “granularity” of experimental measurements, which reflect the scale at which the processes are measured.

The two most important features of collective dynamics in any multicomponent, coupled system are synchrony and spatiotemporal patterns (Murray 1989; Pikovsky *et al* 2001). Here the dynamics exhibited by the “whole” ensemble can be quite different from the individual components’ behaviour (Bertram *et al* 2000). Spatial patterns can also be set up in structured ensembles (e.g. embryos, cardiac tissue) whose length scale spans that of its several components (Bub *et al* 2005). Usually, while making experimental measurements of any observable quantity in a cell population or tissue, a sum total of the concentration is measured from the whole ensemble, as it is difficult to observe the individual variation of product concentrations in each cell. The underlying assumption is that the total concentration measured (output “signal”) will give representative information of the dynamics of the cellular ensemble. The precision of experimental measurements is limited by many factors, such as the response times and the resolution limit of the instruments used, and also on the sampling rate of the measurements. If the instrument has a low time-resolution, we would get the time average of the “signal” concentration around the instant of sampling. Also, experimental measurements are not instantaneous and are made over a range of time. In such cases one can only measure the spatiotemporal average of the product. Thus, experimental measurements in the multicellular ensemble often comprise spatial averages of the variable of interest, which may also be time-averaged around the sampling time. Hence, it is not clear if the different types of spatiotemporal collective dynamics exhibited by a multiscale system can be distinguished, or be borne out by the coarse-grained and averaged measurements done at different spatial and temporal scales.

The focus of this paper is the study of the role of scales of measurement in the faithful description of collective spatiotemporal patterns and processes in a multicellular ensemble. To study this we have taken the following simple theoretical approach. First, we consider a ring of cells as a model for a simple multicellular ensemble, where each cell interacts with the two nearest neighbouring cells in the ring through intercellular diffusion of the end-product of an intracellular biochemical pathway. Our earlier work on this pathway showed that the dynamics of the end-product in each cell is determined by the kinetic and stoichiometric parameters of the intracellular pathway (Sinha and Ramaswamy 1987; Suguna *et al* 1999). The spatiotemporal collective behaviour of the end-product in this model multicellular ensemble (i.e. the ring of cells) was studied for different diffusive coupling strengths and ring size (i.e. the number of cells). It was shown that this ring of cells exhibits different types of global collective dynamics and/or spatial patterns of the end-product concentration under different conditions when studied at the lowest time and space scale, which is not always the same as the individual cell’s dynamics (Suguna and Sinha 2005; Rajesh *et al* 2007). To address the role of resolving power intrinsic to the methods/instruments of measurements in discriminating between the distinctly different collective dynamics of the ring, we now study the role of spatial and temporal averaging of the variable of interest (end-product of the pathway, here) at these different behavioural regimes. We show that the spatiotemporal averaging of these “signals” in different synchronization states can have non-intuitive temporal features, and can either mask the differences, or show a totally different behaviour leading to inconsistent inferences. This has an important bearing in the understanding and prediction of collective functional behaviour in cellular ensembles from experimental data *à vis* theoretical analysis.

2. Models and methods

2.1 Single cell model

Each cell in the model multicellular system, i.e. the ring of cells, incorporates a three-step activator–inhibitor biochemical pathway, where the substrate S1 is converted to S3 through an intermediate substrate S2 (figure 2a). The flux through the pathway is regulated by two feedback loops – the end-product inhibition of S1 by S3 (negative feedback), and the autocatalytic production (positive feedback) of S3 from S2 mediated by an allosteric enzyme E. The details of the model have been studied earlier (Sinha and Ramaswamy 1987; Suguna *et al* 1999).

The time evolution of the three substrates S1, S2 and S3 of the pathway can be described by the following

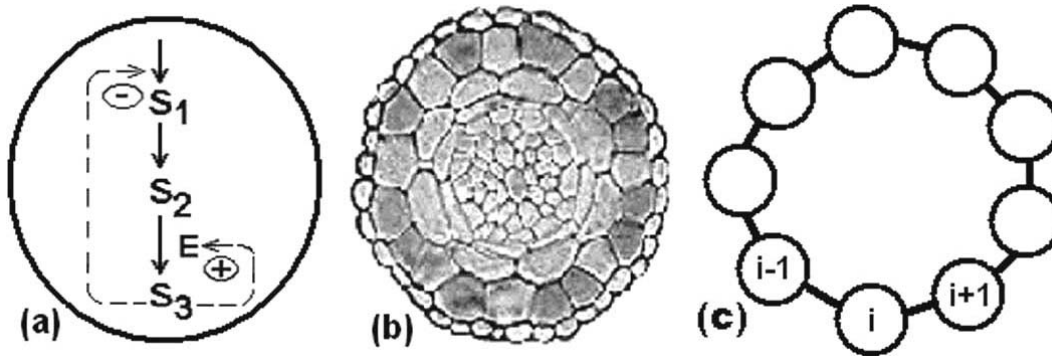


Figure 2. The model multicellular ensemble: (a) A single cell incorporating a three-step biochemical pathway; (b) Circular arrangement of cells in plant root section; (c) A ring of cells where each cell (node i , as shown in [a]) is diffusively coupled to its nearest neighbouring cells (nodes, $i+1$ and $i-1$).

dimensionless equations:

$$\begin{aligned} \frac{dx}{dt} &= F(z) - kx; \\ \frac{dy}{dt} &= x - G(y, z); \\ \frac{dz}{dt} &= G(y, z) - qz, \end{aligned} \tag{1}$$

where x , y and z are the normalized concentrations of the substrates S1, S2 and S3. The first-order, non-saturated rates of the degradation reaction of S1 and S3 are k and q . The non-linear functions $F(z)$ and $G(y, z)$ represent the negative and positive feedback processes and are found to be as follows:

$$F(z) = 1/(1+z^n), \quad G(y, z) = Ty(1+y)(1+z)^2/[L+(1+y)^2(1+z)^2],$$

where L and T are the allosteric constant and maximum velocity of the enzyme E , respectively.

The parameter values used in this model pathway are chosen based on pathways incorporating positive and negative feedback processes such as the cell cycle, glycolytic cycle and cAMP oscillations in slime molds (Goldbeter and Nicolis 1976; Tyson 1983). The basal parameter values are: $n=4$, $L=10^6$, $T=10$, $k=1$, and $q=0.01$, where it shows a simple limit cycle oscillation. The dynamics exhibited by this pathway are a function of the parameters (Suguna *et al* 1999), and the parameters chosen for this study are $q=0.1$, and $k=0.003$, where the end-product dynamics is chaotic (Sinha and Ramaswamy 1987; Suguna and Sinha 2005).

2.2 Model of the multicellular ensemble: ring of cells

For the multicellular ensemble we consider a simple model where the cells are assumed to form a closed ring-like lattice structure, as is observed in cells in a plant root (figure 2b).

Each cell in this one-dimensional lattice of N cells (figure 2c) has the model biochemical pathway described by Eq. (1) (shown in figure 2a), and interacts through the diffusion of a fraction of the end-product z , from each cell (i) to its two neighbouring cells ($i+1$ and $i-1$).

The time evolution of the pathway in this ring of N cells (with periodic boundary conditions) is given by the following equations:

$$\begin{aligned} \frac{dx^i}{dt} &= F(z^i) - kx^i; \\ \frac{dy^i}{dt} &= x^i - G(y^i, z^i) \\ \frac{dz^i}{dt} &= G(y^i, z^i) - qz^i - \epsilon(z^i) + (\epsilon/2)*(z^{i-1} + z^{i+1}), \end{aligned} \tag{2}$$

where ϵ ($0 < \epsilon < 1$) is the diffusive coupling strength of the end-product to its nearest neighbours. The N cells are indexed as $i = 1, \dots, N$.

The spatiotemporal behaviour of this multicell system is simulated using a discretization scheme in the coupled map lattice approach (Oono and Puri 1987; Kaneko 1993). Simulation is done using the fourth-order Runge-Kutta scheme (Press *et al* 1992) and data visualization using MATLAB (<http://www.mathworks.com>). All studies have been carried out with a minimum of fifty different random initial conditions uniformly distributed around the unstable steady state ($z^* \approx 2$, $z^* \approx 5.163$). Simulations have been performed for $t=10^5$, and results are generally presented for the end-product z for the last 5000 time units.

3. Results

In the following sections, we first give a concise description of the pathway behaviour in single cells in the ring when uncoupled. On coupling through diffusion, the collective

behaviour of the cells in the ring depends on the size of the ensemble (N) and the rate of diffusion (ε). We present the spatiotemporal behaviour exhibited by the ring of coupled cells with varying N and ε (for details, see Rajesh *et al* 2007). We then show how different time scales of measurements affect the resolution of the underlying ensemble behaviour at these behavioural regimes.

It may be mentioned here that this pathway exhibits a wide range of dynamics – equilibrium, limit cycle, period-doubling, birhythmic, complex and chaotic oscillations – with variation in parameters, and the complex and chaotic dynamics are observed in a larger parameter space as the cooperativity of negative feedback (n) increases (Suguna *et al* 1999). An earlier study (Suguna and Sinha 2005) with coupled cells at different dynamic regimes showed that (i) the global dynamics in coupled cells are fully synchronized, with the same periodicity and amplitude as the individual oscillatory cells. Thus, the collective dynamics of the coupled cell system is identical to that of a single cell in this regime; and (ii) cells at birhythmic states synchronize to the faster oscillation type for larger lattice size.

3.1 Dynamics of uncoupled cells

For the kinetic parameters chosen, the pathway in each cell exhibits highly irregular, fluctuating, chaotic dynamics in the substrate and end-product concentrations (Suguna *et al* 1999). Figure 3 shows the local and ensemble dynamics of 50 uncoupled cells. Figure 3a shows the (y - z) phase portrait of these irregular oscillations, and figure 3b the broadband nature of the log-power spectrum of the 25th cell on the ring, which is indicative of the diverse time-scales of oscillations associated with the chaotic dynamics. Figure 3c shows the superposition of the time series of the end-product z for all 50 cells. As a result of their sensitivity to initial conditions, a generic property of chaotic oscillations, the time series of z in these cells is totally unsynchronized and uncorrelated. Figure 3d shows the space-time image plot of the uncoupled ensemble, where the X-axis plots the number of cells, and the Y-axis shows the time evolution of z in each cell. The colour bar denotes the value of z . It is clear here that, like figure 3c, cells evolve independently with their intrinsic chaotic dynamics.

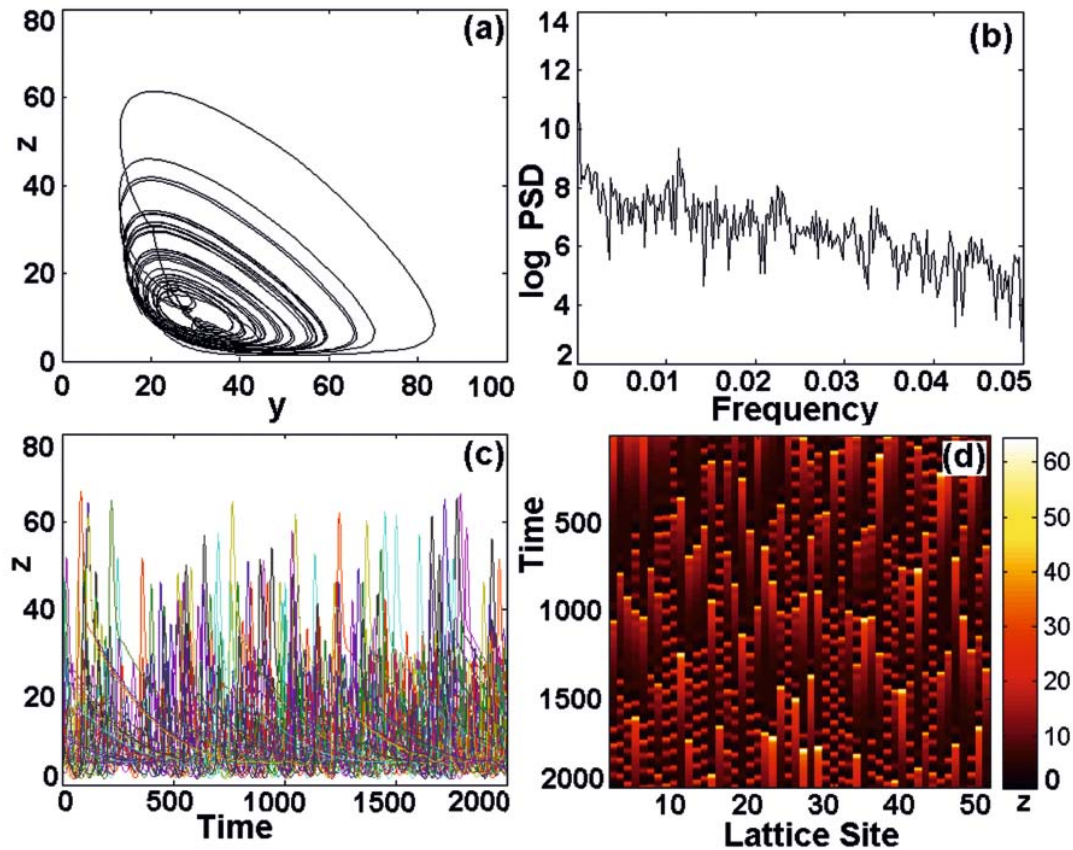


Figure 3. Dynamics of 50 uncoupled cells. (a) (y - z) Phase portrait, and (b) logarithm of the power spectral density of the 25th cell. (c) Superposition of time series, and (d) space-time plot of all the cells.

3.2 Spatiotemporal behaviour of the ring of cells

When these cells exhibiting chaotic dynamics interact with their nearest neighbours in the ring through diffusion of the end-product z , their individual and collective behaviour depends on the size of the ensemble (N) and the rate of diffusion (ϵ). We first show the role of system size (number of cells, N) in the emergent collective behaviour, and then show the spatiotemporal dynamics of the cells for different diffusive strengths (ϵ) for a fixed number of cells in the ring.

3.2.1 Effect of the number cells in the ring (N): To study the different types of collective dynamics exhibited by the ring of cells of different sizes, simulations have been done on lattices of size $N=10$ to 100 in multiples of 10. Two features have been noted while studying how the inclusion of more cells affects the dynamical behaviour of the cells in the ring – the dynamics exhibited by the individual cells in the ring, and the global spatiotemporal behaviour of the ring of cells.

Examples of the different types of collective dynamics exhibited by the ring of cells of different sizes (N) are shown

in figure 4. The left column shows the superposition of time series of z in all the cells. The middle column shows the space–time plot of z with the concentration being colour-coded (colour bar scale shown). To characterize the change in the local dynamics of the cells, the right column shows the major frequency components of the dynamics in one of the cells (cell number= $N/2$) in its power spectrum.

Four types of global dynamics are observed for different N in the ring of cells:

- (i) *Complete synchronization (CS):* For small ring sizes (e.g. $N=10, 20, 30$), all the cells in the ring are completely synchronized in their behaviour – both in phase and amplitude – and they all exhibit chaotic dynamics. Figure 4a shows the superposition of time series plots of 10 cells (for $\epsilon = 0.72$), which gives a single trajectory implying that the concentration of z in all the cells changes in exact synchrony. The space–time plot (figure 4b) also confirms the complete synchronization as z concentrations in all cells in the ring are perfectly in line. The power spectrum (figure 4c) of the 5th cell's time series confirms the chaotic nature of the dynamics through its broadband nature. This indicates that the local and global

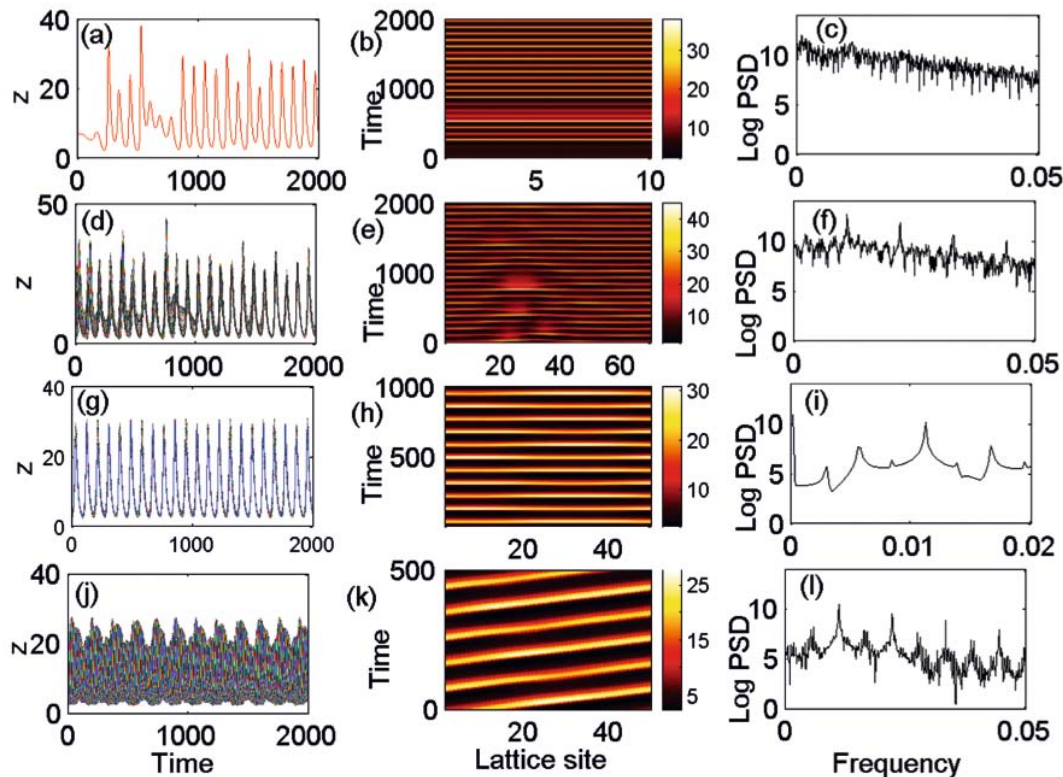


Figure 4. Collective behaviour of coupled cells. *Left column:* superposition of time series of all cells. *Middle column:* space–time image of the ring of cells. *Right column:* Power spectrum of the time series of z of the ($N/2$)th cell in the ring. $\epsilon = 0.72$ for (a–i), and $\epsilon = 0.6$ for (j–l). (a–c) Complete synchronization, $N=10$. (d–f) Intermittent phase synchronization, $N=70$. (g–i) Periodic phase synchronization, $N=50$. (j–l) Travelling wave, $N=50$. ϵ , diffusive coupling strength; z , end-product.

dynamics are the same in small rings of cells, and the ring of cells acts like a coherent ensemble.

- (ii) *Intermittent phase synchronization (IPS)*: For larger size rings, the dynamics of all the cells are not perfectly correlated all the time. The phase synchrony is lost for certain intervals and is regained within a short time. The individual behaviour of the cells remains chaotic. Figure 4d–f illustrates the intermittent behaviour of the ring for $N = 70$ and $\varepsilon = 0.72$. Both the time series plot (figure 4d) and the space–time plot (figure 4e) show that the cells’ dynamics are not perfectly correlated all the time. Here, the cells switch between synchronized and unsynchronized states (intermittency) at irregular intervals. The individual cell’s dynamics are chaotic as seen from the broadband nature of the power spectrum (figure 4f).
- (iii) *Phase synchronization (PS)*: Though IPS is the most common form of global collective dynamics exhibited by larger size rings, occasional cases of other types of dynamics, such as *phase synchronization* and *travelling waves* are also observed for larger ensembles. In figure 4g–i, for $N = 50$, $\varepsilon = 0.72$, the ring of cells exhibits an interesting case of *phase synchronization with phase slip*, where, even though the chaotic dynamics in each cell is completely suppressed, and they show stable periodic (period 4) oscillations, but all the cells in the ring do not oscillate at the same phase instead are phase-locked to be in a synchronized state. There is a phase entrainment with a spatial pattern of phase slips that allows the global dynamics of the ring of cells to be “two high peaks followed by two lower peaks” (see Rajesh *et al* 2007 for details). The superposition of time series plots of all 50 cells is

shown in figure 4g. The space–time plot (figure 4h) and the power spectrum (figure 4i) confirm the phase synchrony and periodic nature of the oscillations. The broadband nature is absent in the power spectrum since chaos has been suppressed and the individual cells show a higher periodic oscillation.

- (iv) *Travelling waves (TW)*: Figure 4j–l shows an example of the other type of collective dynamics – *travelling waves* of the end-product concentration through the ring of cells, for $N = 50$ and $\varepsilon = 0.6$. Here the concentration of z (phases of oscillation) in the cells is distributed throughout the ring as a spatially non-localized structure, such that its spatiotemporal evolution gives rise to a *travelling wave*. The peak of the wave travels through the circular lattice with almost uniform velocity (figure 4k), while the individual cell dynamics remain chaotic (figure 4l).

3.2.2 *Effect of coupling strength ε* : The strength of intercellular interaction also plays a role in determining the collective behaviour of the ring of cells. We studied the spatiotemporal dynamics of a ring of cells ($N=50$) for the range of coupling strengths $0 < \varepsilon < 1$ at a step of 0.1. To include the effects of the intrinsic variability in the intracellular concentrations in different cells, we studied the spatiotemporal dynamics of the ring of cells for 50 different initial values of the pathway metabolites for every ε . Figure 5 shows the collective behaviour exhibited by the ring of cells for different coupling strengths (ε in Y axis) for the 50 initial conditions (in X axis). It is clear from the figure that IPS (in grey) is the predominant collective behaviour at low and medium strengths of diffusive coupling for the ring of 50 cells. But the ring does show PS (in white) with individual cells having periodic dynamics at higher coupling

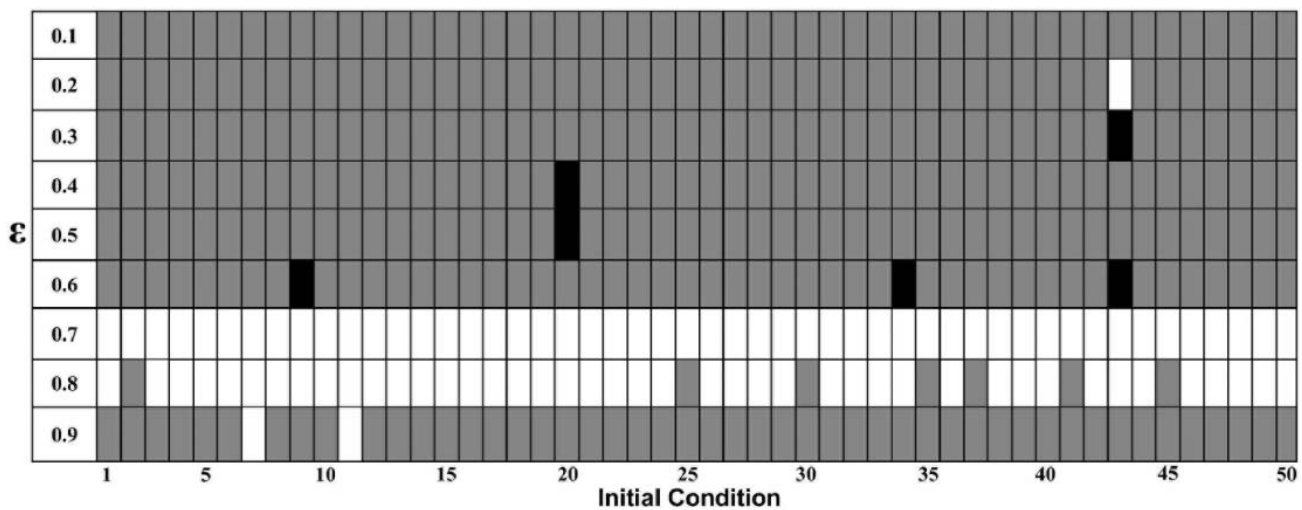


Figure 5. Variety of collective dynamics exhibited by the ring of cells ($N = 50$) for different ε . Colour code for dynamics – grey: IPS; white: PS; black: TW. See text for details. ε , diffusive coupling strength.

strengths ($\varepsilon = 0.7, 0.8$). In a few cases the existence of TW (in black) are also observed. Since complete synchronization (CS) is seen only in rings of small numbers of cells, no such dynamics are observed here.

In all the above cases, the dynamics of z in the individual cells, when coupled in the ring, mostly remains chaotic, and sometimes changes to periodic (period 4 for PS). But the ring of cells, as an ensemble, shows a variety of collective behaviours as is seen in figure 4. Thus, the effect of intercellular diffusion can lead to the setting up of different types of global spatiotemporal dynamical patterns spanning different space and time scales in multicellular ensembles of different sizes. Such interaction in an ensemble can also induce changes in the local dynamics of the individual cells from chaotic to periodic, thereby suppressing the intrinsic behaviour of the cells.

3.3 Measuring collective behaviour

Through simulation we can track the concentration of the end-product (z) in the individual cells and also for the ring of cells at different dynamical states. Here we address the role of the resolving power of experimental measurements in

discriminating between these distinctly different collective dynamics of the ring. Generally, experimental measurements of z in the ring of cells would involve sampling of the total amount of z (“signal” or “output”) from the cells at scales that are limited by the instrumental precision and measurement protocols. Thus, experimental measurements on the ring would comprise spatial averages of z , which may also be time-averaged around the sampling time. In the following sections we study these two experimentally relevant features – spatial averaging and spatiotemporal averaging of measurements of the concentrations of z in the ring of cells – at different collective dynamical regimes as shown in figure 4 (CS, IPS, PS, TW) along with the uncoupled cells (figure 3).

3.3.1 Measuring the total output “signal”: The time series of the spatial average of z , Z_{av} , is plotted in figure 6 for the uncoupled and coupled cells in the ring at different behavioural regimes. This would represent the total “output signal” of z from the multicellular ensemble at different spatiotemporal dynamical states. Measurements have been done at every time step of simulations here.

Figure 6a shows that even though each cell in the uncoupled cell population shows large and irregular

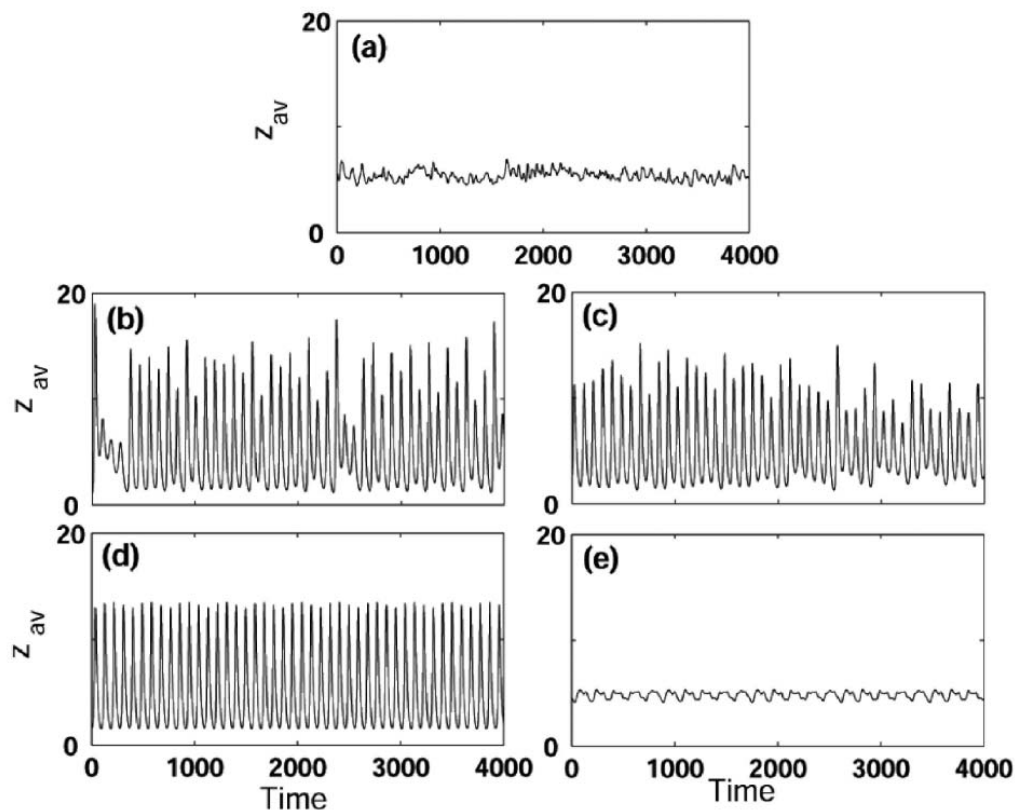


Figure 6. Time evolution of total output (Z_{av}). (a) Uncoupled chaotic cells; (b) Complete synchronized state; (c) Intermittent phase synchronized state; (d) Periodic synchronized state; (e) Travelling wave.

concentration changes of z , the ensemble output of z is relatively steady. This is because the concentration variation of z in the cells is phase incoherent and asynchronous. Thus, the underlying chaotic dynamics in the individual cells are not measurable from the total output signal, which shows small fluctuations around the mean value. The “output” of z shown in figure 6b, c, on the other hand, is almost indistinguishable, even though the underlying spatiotemporal dynamics of the ring of coupled cells are in CS or IPS. Figure 6d shows that the average output from the ring when the cell dynamics are in PS is not different from the spatiotemporal behaviour seen in figure 4g. In the TW state, when there is a chaotic travelling wave front moving through the ring, Z_{av} shows a totally different temporal behaviour (figure 6e). The high amplitude variation in z (figure 4i) is completely suppressed, and a very small-amplitude oscillation around 10 units is obtained in this case. The temporal behaviour of the Z_{av} in the uncoupled (figure 6a) and coupled cells undergoing TW dynamics (figure 6e) show a similar trend. Thus, from figure 6, it is clear that the total “output signal” of the multicell ensemble may not be representative of either single-cell

behaviour or the collective spatiotemporal dynamics, and the spatiotemporal pattern and dynamics cannot be easily distinguished by measuring the spatial average of the ensemble of cells.

3.3.2 Role of time scales in the measurement of the spatial average of z : The precision of experimental measurements is limited by the response times of the instruments and by the sampling rate of the experimenter. At low temporal resolution, one gets the time average of Z_{av} in the ensemble around the sampling instant. In such cases one can only measure the spatiotemporal average of the end-product for a time range. In general, as expected, fluctuations tend to smoothen out as the time scale of averaging is increased, since the small-scale variations in the time series are lost. In figures 7–9, we show the time series of the output signal (Z_{av}) after averaging over different time intervals (50, 100 and 500 time units), for the five collective dynamical states – uncoupled, CS, IPS, PS and TW.

For a short sampling time (50 units in figure 7), the temporal variations of Z_{av} are almost indistinguishable

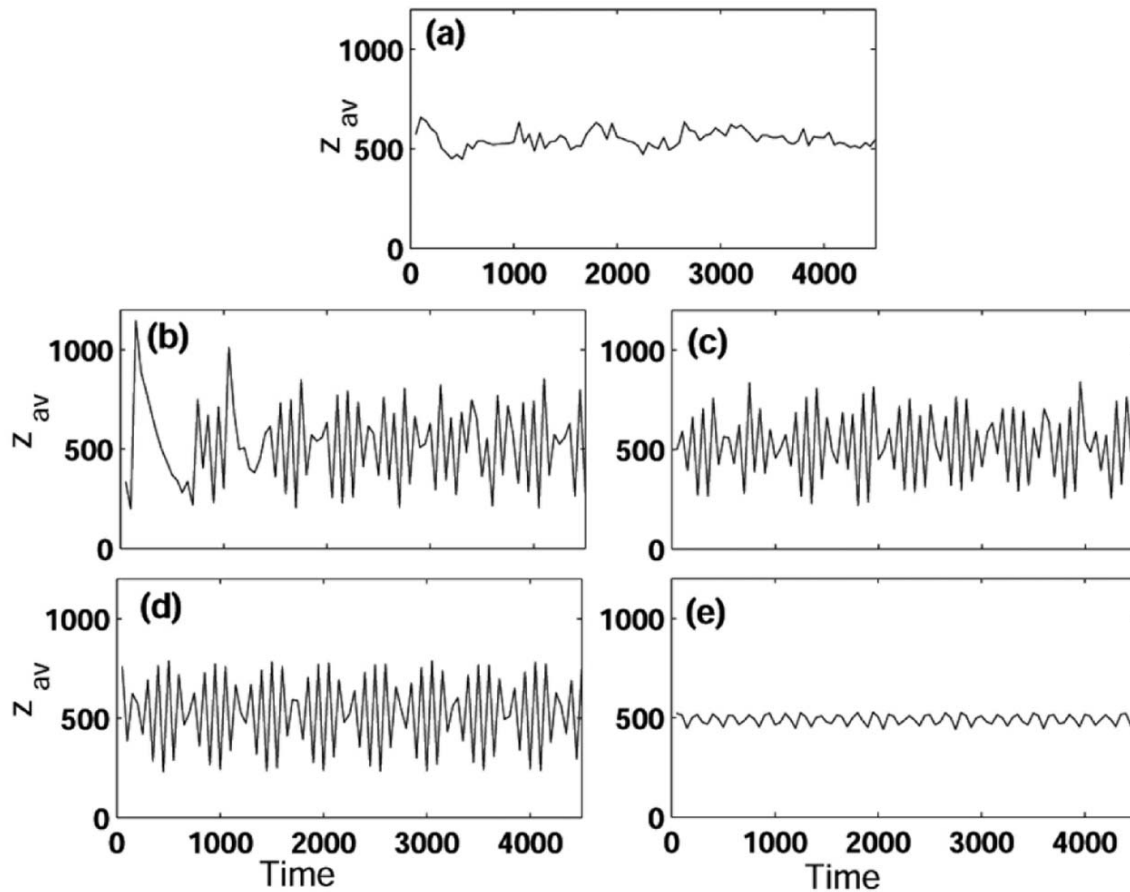


Figure 7. Time evolution of output (Z_{av}) averaged over 50 time units: (a) Uncoupled chaotic cells; (b) Complete synchronized state; (c) Intermittent phase synchronized state; (d) Periodic synchronized state; (e) Travelling wave.

for CS, IPS and PS (figure 7b, c, d), except the feature that the ring of cells showing CS can sometimes show a large amplitude pulse of the output signal due to their synchronized chaotic dynamics. Z_{av} in both uncoupled cells and coupled cells in TW exhibits a rather regular output of the same value with small fluctuations around the mean.

At larger sampling times (100 in figure 8 and 500 in figure 9), the temporal dynamics of the “output signal” from the ring at CS, IPS and PS continue to show similar behaviour and tend to be similar to the uncoupled cells, except that the signals from PS show more regular oscillations and those from CS exhibit occasional bursts. The ring showing TW dynamics gives a fairly constant regular output of Z_{av} , even though it is shown earlier that the individual cells show chaotic oscillations and the collective behaviour has concentration waves travelling along the ring.

Thus, our results show that the four different spatio-temporal dynamical states cannot be easily distinguished from the spatially averaged and spatiotemporally averaged measurements of the “output signal”. This is clearly seen when the ring of cells shows the non-stationary structure of TW (compare figure 4i with figures 6e, 7e, 8e and

9e), where the large oscillation in the local temporal and global spatiotemporal dynamics are completely suppressed in the population average measurements, giving only a near-constant regular output. The multicellular rings with completely synchronized (figures 7b, 8b and 9b) and intermittently synchronized (figures 7c, 8c and 9c) dynamics tend to show indistinguishable temporal behaviour of the total “signal”, except for the existence of sudden “high” in the former. In fact, for medium and high temporal averaging (100 and 500), the three different dynamical states of the lattice – CS, IPS and PS – cannot be easily distinguished from the uncoupled cells in their total spatiotemporal output. The phase-synchronized periodic ring shows interesting transitions depending on the time range of sampling. It shows a burst-like behaviour for both low and high temporal averages (figures 7d and 9d), but exhibits a fairly regular output for medium temporal averaging (figure 8d). Thus, the temporal behaviour of the total output “signal” from the multicell ensemble may not faithfully represent its underlying spatiotemporal collective dynamics, and can exhibit different behaviour depending on the time of sampling.

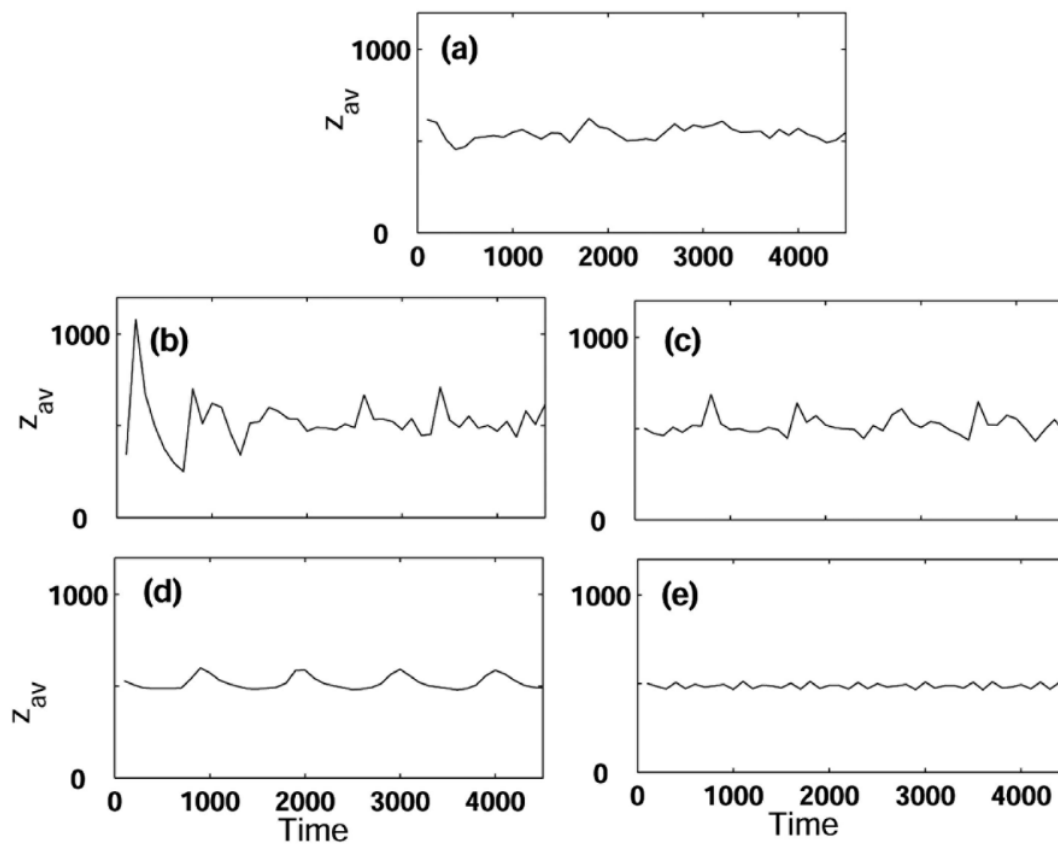


Figure 8. Time evolution of output (Z_{av}) averaged over 100 time units: (a) Uncoupled chaotic cells; (b) Complete synchronized state; (c) Intermittent phase synchronized state; (d) Periodic synchronized state; (e) Travelling wave.

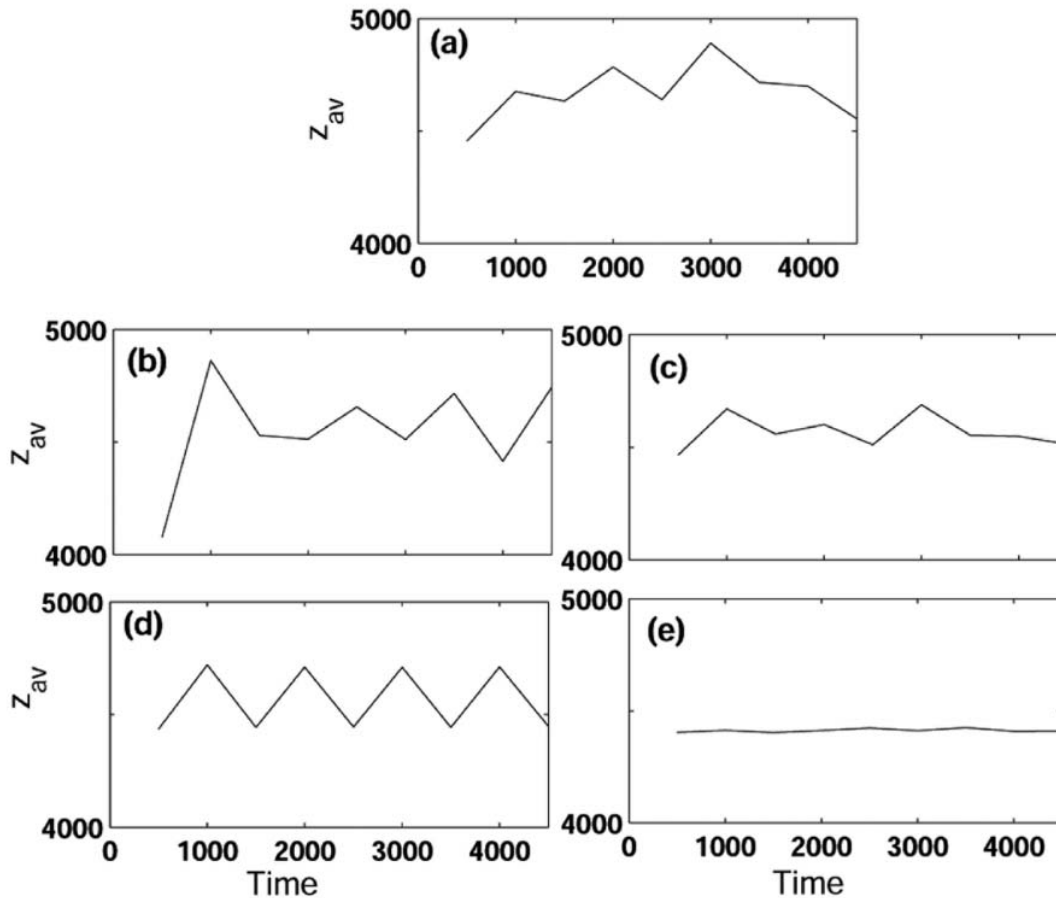


Figure 9. Time evolution of output (Z_{av}) averaged over 500 time units: (a) Uncoupled chaotic cells; (b) Complete synchronized state; (c) Intermittent phase synchronized state; (d) Periodic synchronized state; (e) Travelling wave.

4. Discussion

It is increasingly becoming apparent that many biological mechanisms act at various spatiotemporal scales in multicellular organisms, which require multiscale and multilevel measurements and modelling methods (Alber *et al* 2005; Chaturvedi *et al* 2005). Most studies (experimental, modelling and simulation) have focused on single levels or scales, e.g. genomic/proteomic, cellular, tissue, organ, whole body, etc. But each of these contains processes/components that span multiple lengths and time scales – from nanometers to meters and from nanoseconds to days, months and longer. The number of components can also be large (thousands of interacting molecules and ions) with non-linear and stochastic interactions among them. Spatiotemporal patterns and collective dynamics are important features of complex multicellular processes/systems in normal and diseased conditions, such as embryonic development, cancer, quorum sensing, cardiac rhythm, which happen over many space and time scales (Glass 2001). Interesting synchronization

patterns are found in ecological systems as well. Here, migration among population patches leads to broad-scale PS with the peak population abundances remaining largely uncorrelated. This can lead to the emergence of complex TW structures, which may be crucial for species persistence (Blasius *et al* 1999). Thus, the overall collective behaviour in biological systems is an emergent property of the processes occurring at different scales.

We have shown with a simple model that much of the smaller- and larger-scale information of spatial pattern and collective dynamics may be lost or remain unresolved due to the coarseness or granularity of the measurement schemes. The intrinsic resolution scale that decides the reliability of measurement can lead to incorrect and ambiguous inferences about system behaviour and can influence the predictive capability of the experiments at other scales. Similar problems have been discussed even in theoretical methods where detection of modularity in social, biological and physical networks to study community structures are limited by the detection algorithm (Fortunato and Barthélemy 2007).

To address this, modellers are developing software tools and mathematical approaches to integrate data and models from microscales to macroscales in a seamless fashion. Such multiscale models are essential if we are to produce quantitative, predictive models of complex biological behaviours. In experiments, recent advances in measurement technology, such as large-scale gene expression, protein profiling, high-throughput microscale imaging and ultrafast temporal measurements, along with intracellular measurements at single-cell level in a population (Golding *et al* 2005; Rosenfeld *et al* 2005; Auer *et al* 2007) have not only significantly aided the concurrent study of a large number of interacting components underlying cellular functions, but are also allowing observations to be made at milli-, micro- and nanometer space scales to study biological processes as they unfold. As is shown in figure 1, this would certainly improve the mining of information at different scales of resolution and complexity, and lead to a much deeper understanding of the physiological functions and pathogenesis in multicell ensembles, for both basic and applied sciences.

Acknowledgements

SS thanks Gene Myers for sharing the results given in figure 1, and R R Sarkar for critical reading of the manuscript. SS also thanks the Wissenschaftskolleg at Berlin for the fellowship during which the work was conceived.

References

- Alarcon T, Byrne H M and Maini P K 2005 A multiple scale model for tumor growth; *Multiscale Model. Simul.* **3** 440–475
- Alber M, Hou T, Glazier J A and Jiang Y (Guest editors) 2005 Special issue on multiscale modeling in biology; *Multiscale Model. Simul.* **3** vii–viii
- Auer M, Peng H and Singh A 2007 Development of multiscale biological image data analysis: review of 2006 International workshop on multiscale biological imaging, data mining and informatics, Santa Barbara, USA (BII06); *BMC Cell Biol.* **8** doi: 10.1186/1471-2121-8-S1-S1
- Bertram R, Previte J, Sherman A, Kinard T A and Satin L S 2000 The phantom burster model for pancreatic beta-cells; *Biophys. J.* **79** 2880–2892
- Blasius, B, Huppert A and Stone L 1999 Complex dynamics and phase synchronization in spatially extended ecological systems; *Nature (London)* **399** 354–359
- Bub G, Shrier A and Glass L 2005 Global organization of dynamics in heterogeneous, spontaneously active excitable media; *Phys. Rev. Lett.* **94** 028105 (1–4)
- Chaturvedi R, Huang C, Kazmierczak B, Schneider T, Izaguirre J A, Glimm T, Hentschel H G E, Glazier J A, Newman S A and Alber M S 2005 On multiscale approaches to three-dimensional modelling of morphogenesis; *J. R. Soc. Interface* **2** 237–253
- Costerton J W 2004 A short history of the development of the biofilm concept; in *Microbial biofilms* (eds) M A Ghannoum and G O'Toole (Washington DC: ASM Press) pp 4–19
- Erban R and Othmer H 2005 From signal transduction to spatial pattern formation in *E. coli*: a paradigm for multi-scale modeling in biology; *Multiscale Model. Simul.* **3** 362–394
- Fortunato S and Barthélemy M 2007 Resolution limit in community detection; *Proc. Natl. Acad. Sci. USA* **104** 36–41
- Freeman M and Gurdon J B 2002 Regulatory principles of developmental signalling; *Annu. Rev. Cell Dev. Biol.* **18** 515–539
- Fuqua C, Winans S C and Greenberg E P 1996 Quorum sensing in bacteria: the LuxR/LuxI family of cell density-responsive transcriptional regulators; *Annu. Rev. Microbiol.* **50** 727–751
- Garcia A L, Bell J B, Crutchfield W Y and Alder B J 1999 Adaptive mesh and algorithm refinement using direct simulation Monte Carlo; *J. Comput. Phys.* **154** 134–155
- Garcia-Ojalvo J, Elowitz M B and Strogatz S H 2004 Modeling a synthetic multicellular clock: repressilators coupled by quorum sensing; *Proc. Natl. Acad. Sci. USA* **101** 10955–10960
- Glass L 2001 Synchronization and rhythmic processes in physiology; *Nature (London)* **410** 277–284
- Goldbeter A and Nicolis G 1976 An allosteric enzyme model with positive feedback applied to glycolytic oscillations; *Prog. Theor. Biol.* **4** 65–160
- Golding I, Paulsson J, Zawilski S M and Cox E C 2005 Real-time kinetics of gene activity in individual bacteria; *Cell* **123** 1025–1036
- Kaneko K (ed.) 1993 *Theory and applications of coupled map lattices* (New York: Wiley)
- Kevrekidis I G, Gear C W, Hyman J M, Kevrekidis P G, Runborg O and Theodoropoulos K 2003 Equation-free multiscale computation: enabling microscopic simulators to perform system-level tasks; *Commun. Math. Sci.* **1** 715–762
- Kevrekidis I G, Gear C W and Hummer G 2005 Equation-free modeling for complex systems; in *Frontiers of engineering: reports on leading-edge engineering from the 2004 NAE symposium on frontiers of engineering* (Washington: The National Academies Press) pp 69–76
- Maithreye R and Sinha S 2007 Propagation of extrinsic perturbation in a negatively auto-regulated pathway; *Phys. Biol.* **4** 48–59
- Miller M B and Bassler B L 2001 Quorum sensing in bacteria; *Annu. Rev. Microbiol.* **55** 165–199
- Murray J D 1989 *Mathematical biology* (Berlin: Springer-Verlag)
- Oono Y and Puri S 1987 Computationally efficient modeling of ordering of quenched phases; *Phys. Rev. Lett.* **58** 836–840
- Peng H, Long F, Zhou J, Leung G, Eisen M B and Myers E W 2007 Automatic image analysis for gene expression patterns of fly embryos; *BMC Cell Biol. (Suppl. 1)*: **8** S7 doi: 10.1186/1471-2121-8-S1-S7.
- Pikovsky A, Rosenblum M and Kurths J 2001 *Synchronization: a universal concept in nonlinear sciences* (Cambridge: Cambridge University Press)
- Press W H, Teukolsky S A, Vetterling W T and Flannery B P 1992 *Numerical recipes in C* (Cambridge: Cambridge University Press)
- Rajesh S, Sinha S and Sinha S 2007 Synchronization in coupled cells with activator–inhibitor pathways; *Phys. Rev. E* **75** 011906 (1–11)

- Rosenfeld N, Young J W, Alon U, Swain P S and Elowitz M B 2005 Gene regulation at the single-cell level; *Science* **307** 1962–1965
- Setayeshgar S, Gear C W, Othmer H G and Kevrekidis I G 2005 Application of coarse integration to bacterial chemotaxis; *Multiscale Model. Simul.* **4** 307–327
- Shenoy V B, Miller R, Tadmor E B, Rodney D, Phillips R and Ortiz M 1999 An adaptive finite element approach to atomic-scale mechanics – the quasi-continuum method; *J. Mech. Phys. Solids* **47** 611–642
- Sinha S 2005 Multiplicity in non-linear systems; in *Understanding change: models, methodologies and metaphors* (eds) A Wimmer and R Kössler (Basingstoke: Palgrave Macmillan) pp 222–235
- Sinha S and Ramaswamy R 1987 On the dynamics of controlled metabolic network and cellular behaviour; *Biosystems* **20** 341–354
- Suguna C, Chowdhury K K and Sinha S 1999 Minimal model for complex dynamics in cellular processes; *Phys. Rev. E* **60** 5943–5949
- Suguna C and Sinha S 2005 Dynamics of coupled-cell systems; *Physica A* **346** 154–164
- Tyson J J 1983 Periodic enzyme synthesis and oscillatory repression. Why is the period of oscillation close to cell cycle?; *J. Theor. Biol.* **103** 313–328

MS received 10 September 2007; accepted 7 February 2008

ePublication: 13 March 2008

Corresponding editor: ALBERT GOLDBETER